

Regularized Principal Component Analysis for Spatial Data

Wen-Ting Wang
Institute of Statistics
National Chiao Tung University
egpivo@gmail.com
and
Hsin-Cheng Huang
Institute of Statistical Science
Academia Sinica
hchuang@stat.sinica.edu.tw

Abstract: In many atmospheric and earth sciences, it is of interest to identify dominant spatial patterns of variation based on data observed at p locations and n time points with the possibility that $p > n$. While principal component analysis (PCA) is commonly applied to find the dominant patterns, the eigenimages produced from PCA may exhibit patterns that are too noisy to be physically meaningful when p is large relative to n . To obtain more precise estimates of eigenimages, we propose a regularization approach incorporating smoothness and sparseness of eigenimages, while accounting for their orthogonality. Our method allows data taken at irregularly spaced or sparse locations. In addition, the resulting optimization problem can be solved using the alternating direction method of multipliers, which is easy to implement, and applicable to a large spatial dataset. Furthermore, the estimated eigenfunctions provide a natural basis for representing the underlying spatial process in a spatial random-effects model, from which spatial covariance function estimation and spatial prediction can be efficiently performed using a regularized fixed-rank kriging method. Finally, the effectiveness of the proposed method is demonstrated by several numerical examples.

Keywords: Alternating direction method of multipliers, empirical orthogonal functions, fixed rank kriging, Lasso, non-stationary spatial covariance estimation, orthogonal constraint, smoothing splines.

1. Introduction

In many atmospheric and earth sciences, it is of interest to identify dominant spatial patterns of variation based on data observed at p locations with n repeated measurements, where p may be larger than n . The dominant patterns are the eigenimages of the underlying (nonstationary) spatial covariance function with large eigenvalues. A commonly used approach for estimating the eigenimages is the principal component analysis (PCA), also known as the empirical orthogonal function analysis in atmospheric science. However, when p is large relative to n , the leading eigenimages produced from PCA may be noisy with high estimation variability, or exhibit some bizarre patterns that are not physically meaningful. To enhance the interpretability, a few approaches, such as rotation of components according to some criteria (see [Richman \(1986\)](#), [Jolliffe \(1987\)](#), [Richman \(1987\)](#)), have been proposed to form more desirable patterns. However, how to obtain a desired rotation in practice is not completely clear. Some discussion can be found in [Hannachi, Jolliffe and Stephenson \(2007\)](#).

Another approach to aid interpretation is to seek sparse or spatially localized patterns, which can be done by imposing an L_1 constraint or adding an L_1 penalty to an original PCA optimization formulation ([Jolliffe, Uddin and Vines \(2002\)](#), [Zou, Hastie and Tibshirani \(2006\)](#), [Shen and Huang \(2008\)](#), [d'Aspremont, Bach and Ghaoui \(2008\)](#), and [Lu and Zhang \(2012\)](#)). However, this approach may produce a pattern with isolated zero and nonzero components, and except [Jolliffe, Uddin and Vines \(2002\)](#) and [Lu and Zhang \(2012\)](#), the PC estimates produced from these approaches may not have orthogonal PC loadings.

For continuous spatial domains, the problem becomes even more challenging. Instead of looking for eigenimages on a lattice, we need to find eigenfunctions by essentially solving an infinite dimensional problem based on data observed at possibly sparse and irregularly spaced locations. Although some approaches have been developed using functional principal component analysis (see e.g., [Ramsay and Silverman](#)

(2005), Yao, Muller and Wang (2005) and Huang, Shen and Buja (2008)), they typically focus on one-dimensional processes, or require data observed at dense locations. In particular, these methods generally do not work well when data are observed at fixed but sparse locations. Reviews of PCA on spatial data can be found in Hannachi, Jolliffe and Stephenson (2007) and Demsar et al. (2013).

In this research, we propose a regularization approach for estimating the dominant patterns, taking into account smoothness and localized features that are expected in real-world spatial processes. The proposed estimates are directly obtained by solving a minimization problem. We call our method *SpatPCA*, which not only gives effective estimates of dominant patterns, but also provides an ideal set of basis functions for estimating the underlying (nonstationary) spatial covariance function, even when data are irregularly or sparsely located in space. In addition, we develop a fast algorithm to solve the resulting optimization problem using the alternating direction method of multipliers (ADMM) (see Boyd et al. (2011)). An R package called *SpatPCA* is developed and available on the Comprehensive R Archive Network (CRAN).

The rest of this paper is organized as follows. In Section 2, we introduce the proposed *SpatPCA* method, including dominant patterns estimation and spatial covariance function estimation. Our ADMM algorithm for computing the *SpatPCA* estimates is provided in Section 3. Some simulation experiments that illustrate the superiority of *SpatPCA* and an application of *SpatPCA* to a global sea surface temperature dataset are presented in Section 4.

2. The Proposed Method

Consider a sequence of zero-mean L^2 -continuous spatial processes, $\{\eta_i(\mathbf{s}); \mathbf{s} \in D\}$; $i = 1, \dots, n$, defined on a spatial domain $D \subset \mathbb{R}^d$, which are mutually uncorrelated, and have a common spatial covariance function, $C_\eta(\mathbf{s}, \mathbf{s}^*) = \text{cov}(\eta_i(\mathbf{s}), \eta_i(\mathbf{s}^*))$. We

consider a rank- K spatial random-effects model for $\eta_i(\cdot)$:

$$\eta_i(\mathbf{s}) = (\varphi_1(\mathbf{s}), \dots, \varphi_K(\mathbf{s}))\boldsymbol{\xi}_i = \sum_{k=1}^K \xi_{ik}\varphi_k(\mathbf{s}); \quad \mathbf{s} \in D, \quad i = 1, \dots, n,$$

where $\{\varphi_k(\cdot)\}$ are unknown orthonormal basis functions, $\boldsymbol{\xi}_i = (\xi_{i1}, \dots, \xi_{iK})' \sim (0, \boldsymbol{\Lambda})$; $i = 1, \dots, n$, are uncorrelated random variables, and $\boldsymbol{\Lambda}$ is an unknown symmetric nonnegative-definite matrix, denoted by $\boldsymbol{\Lambda} \succeq \mathbf{0}$. A similar model based on given $\{\varphi_k(\cdot)\}$ was introduced by [Cressie and Johannesson \(2008\)](#) and in a Bayesian framework by [Kang and Cressie \(2011\)](#).

Let $\lambda_{kk'}$ be the (k, k') -th entry of $\boldsymbol{\Lambda}$. Then the spatial covariance function of $\eta_i(\cdot)$ is:

$$C_\eta(\mathbf{s}, \mathbf{s}^*) = \text{cov}(\eta_i(\mathbf{s}), \eta_i(\mathbf{s}^*)) = \sum_{k=1}^K \sum_{k'=1}^K \lambda_{kk'} \varphi_k(\mathbf{s}) \varphi_{k'}(\mathbf{s}^*). \quad (1)$$

Note that $\boldsymbol{\Lambda}$ is not restricted to be a diagonal matrix.

Let $\boldsymbol{\Lambda} = \mathbf{V}\boldsymbol{\Lambda}^*\mathbf{V}'$ be the eigen-decomposition of $\boldsymbol{\Lambda}$, where \mathbf{V} consists of K orthonormal eigenvectors, and $\boldsymbol{\Lambda}^* = \text{diag}(\lambda_1^*, \dots, \lambda_K^*)$ consists of eigenvalues with $\lambda_1^* \geq \dots \geq \lambda_K^*$. Let $\boldsymbol{\xi}_i^* = \mathbf{V}'\boldsymbol{\xi}_i$ and

$$(\varphi_1^*(\mathbf{s}), \dots, \varphi_K^*(\mathbf{s})) = (\varphi_1(\mathbf{s}), \dots, \varphi_K(\mathbf{s}))\mathbf{V}; \quad \mathbf{s} \in D.$$

Then $\varphi_k^*(\cdot)$'s are also orthonormal, and $\xi_{ik}^* \sim (0, \lambda_k^*)$; $i = 1, \dots, n$, $k = 1, \dots, K$, are mutually uncorrelated. Therefore, we can rewrite $\eta_i(\cdot)$ in terms of $\varphi_k^*(\cdot)$'s:

$$\eta_i(\mathbf{s}) = (\varphi_1^*(\mathbf{s}), \dots, \varphi_K^*(\mathbf{s}))\boldsymbol{\xi}_i^* = \sum_{k=1}^K \xi_{ik}^* \varphi_k^*(\mathbf{s}); \quad \mathbf{s} \in D. \quad (2)$$

The above expansion is known as the Karhunen-Loève expansion of $\eta_i(\cdot)$ ([Karhunen \(1947\)](#); [Loève \(1978\)](#)) with K nonzero eigenvalues, where $\varphi_k^*(\cdot)$ is the k -th eigenfunction of $C_\eta(\cdot, \cdot)$ with λ_k^* the corresponding eigenvalue.

Suppose that we observe data $\mathbf{Y}_i = (Y_i(\mathbf{s}_1), \dots, Y_i(\mathbf{s}_p))'$ with added white noise $\boldsymbol{\epsilon}_i \sim (\mathbf{0}, \sigma^2 \mathbf{I})$ at p spatial locations, $\mathbf{s}_1, \dots, \mathbf{s}_p \in D$, according to

$$\mathbf{Y}_i = \boldsymbol{\eta}_i + \boldsymbol{\epsilon}_i = \boldsymbol{\Phi}\boldsymbol{\xi}_i + \boldsymbol{\epsilon}_i; \quad i = 1, \dots, n, \quad (3)$$

where $\boldsymbol{\eta}_i = (\eta_i(\mathbf{s}_1), \dots, \eta_i(\mathbf{s}_p))'$, $\boldsymbol{\Phi} = (\boldsymbol{\phi}_1, \dots, \boldsymbol{\phi}_K)$ is a $p \times K$ matrix with the (j, k) -th entry $\varphi_k(\mathbf{s}_j)$, and $\boldsymbol{\epsilon}_i$'s and $\boldsymbol{\xi}_i$'s are uncorrelated. Our goal is to identify the first $L \leq K$ dominant patterns, $\varphi_1(\cdot), \dots, \varphi_L(\cdot)$, with relatively large $\lambda_1^*, \dots, \lambda_L^*$. Additionally, we are interested in estimating $C_\eta(\cdot, \cdot)$, which is essential for spatial prediction.

Let $\mathbf{Y} = (\mathbf{Y}_1, \dots, \mathbf{Y}_n)'$ be the $n \times p$ data matrix. Throughout the paper, we assume that the mean of \mathbf{Y} is known as zero. So the sample covariance matrix of \mathbf{Y} is $\mathbf{S} = \mathbf{Y}'\mathbf{Y}/n$. A popular approach for estimating $\{\varphi_k^*(\cdot)\}$ is PCA, which estimates $(\varphi_k^*(\mathbf{s}_1), \dots, \varphi_k^*(\mathbf{s}_p))'$ by $\tilde{\boldsymbol{\phi}}_k$, the k -th eigenvector of \mathbf{S} , for $k = 1, \dots, K$. Let $\tilde{\boldsymbol{\Phi}} = (\tilde{\boldsymbol{\phi}}_1, \dots, \tilde{\boldsymbol{\phi}}_K)$ be a $p \times K$ matrix formed by the first K principal component loadings. Then $\tilde{\boldsymbol{\Phi}}$ solves the following constrained optimization problem:

$$\min_{\boldsymbol{\Phi}} \|\mathbf{Y} - \mathbf{Y}\boldsymbol{\Phi}\boldsymbol{\Phi}'\|_F^2 \quad \text{subject to } \boldsymbol{\Phi}'\boldsymbol{\Phi} = \mathbf{I}_K,$$

where $\boldsymbol{\Phi} = (\boldsymbol{\phi}_1, \dots, \boldsymbol{\phi}_K)$ and $\|\mathbf{M}\|_F = \left(\sum_{i,j} m_{ij}^2\right)^{1/2}$ is the Frobenius norm of a matrix \mathbf{M} . Unfortunately, $\tilde{\boldsymbol{\Phi}}$ tends to have high estimation variability when p is large (leading to excessive number of parameters), n is small, or σ^2 is large. Consequently, the patterns of $\tilde{\boldsymbol{\Phi}}$ may be too noisy to be physically interpretable. In addition, for a continuous spatial domain D , we also need to estimate $\varphi_k^*(\mathbf{s})$'s for locations with no data observed (i.e., $\mathbf{s} \notin \{\mathbf{s}_1, \dots, \mathbf{s}_p\}$); see some discussion in Section 12.4 and 13.6 of [Jolliffe \(2002\)](#).

2.1. Regularized Spatial PCA

To prevent high estimation variability of PCA, we adopt a regularization approach by minimizing the following objective function:

$$\|\mathbf{Y} - \mathbf{Y}\boldsymbol{\Phi}\boldsymbol{\Phi}'\|_F^2 + \tau_1 \sum_{k=1}^K J(\varphi_k) + \tau_2 \sum_{k=1}^K \sum_{j=1}^p |\varphi_k(\mathbf{s}_j)|, \quad (4)$$

over $\varphi_1(\cdot), \dots, \varphi_K(\cdot)$, subject to $\boldsymbol{\Phi}'\boldsymbol{\Phi} = \mathbf{I}_K$ and $\boldsymbol{\phi}'_1\mathbf{S}\boldsymbol{\phi}_1 \geq \boldsymbol{\phi}'_2\mathbf{S}\boldsymbol{\phi}_2 \geq \dots \geq \boldsymbol{\phi}'_K\mathbf{S}\boldsymbol{\phi}_K$,

where

$$J(\varphi) = \sum_{z_1 + \dots + z_d = 2} \int_{\mathcal{R}^d} \left(\frac{\partial^2 \varphi(\mathbf{s})}{\partial x_1^{z_1} \dots \partial x_d^{z_d}} \right)^2 d\mathbf{s},$$

is a roughness penalty, $\mathbf{s} = (x_1, \dots, x_d)'$, $\tau_1 \geq 0$ is a smoothness parameter, and $\tau_2 \geq 0$ is a sparseness parameter. The objective function (4) consists of two penalty terms. The first one is designed to enhance smoothness of $\varphi_k(\cdot)$ through the smoothing spline penalty $J(\varphi_k)$, while the second one is the L_1 Lasso penalty (Tibshirani (1996)), used to promote sparse patterns by shrinking some PC loadings to zero. While the L_1 penalty alone may lead to isolated zero and nonzero components with no global feature, when it is paired with the smoothness penalty, local sparsity translates into global sparsity, resulting in connected zero and nonzero patterns. Hence the two penalty terms together lead to desired patterns that are not only smooth but also localized. Specifically, when τ_1 is larger, $\hat{\varphi}_k(\cdot)$'s tend to be smoother and *vice versa*. When τ_2 is larger, $\hat{\varphi}_k(\cdot)$'s are forced to be zero at some $\mathbf{s} \in D$. On the other hand, when both τ_1 and τ_2 are close to zero, the estimates are close to those obtained from PCA. By suitably choosing τ_1 and τ_2 , we can obtain a good compromise among goodness of fit, smoothness of the eigenfunctions, and sparseness of the eigenfunctions, leading to more interpretable results. Note that due to computational difficulty, the orthogonal constraint, is not considered by many PCA regularization methods (e.g., Zou, Hastie and Tibshirani (2006), Shen and Huang (2008), Guo et al. (2010), Hong and Lian (2013)).

Although $J(\varphi)$ involves integration, it is well known from the theory of smoothing splines (Green and Silverman (1994)) that for each $k = 1, \dots, K$, $\hat{\varphi}_k(\cdot)$ has to be a natural cubic spline when $d = 1$, and a thin-plate spline when $d \in \{2, 3\}$ with nodes at $\{\mathbf{s}_1, \dots, \mathbf{s}_p\}$. Specifically,

$$\hat{\varphi}_k(\mathbf{s}) = \sum_{i=1}^p a_i g(\|\mathbf{s} - \mathbf{s}_i\|) + b_0 + \sum_{j=1}^d b_j x_j, \quad (5)$$

where $\mathbf{s} = (x_1, \dots, x_d)'$,

$$g(r) = \begin{cases} \frac{1}{16\pi} r^2 \log r; & \text{if } d = 2, \\ \frac{\Gamma(d/2 - 2)}{16\pi^{d/2}} r^{4-d}; & \text{if } d = 1, 3, \end{cases}$$

and the coefficients $\mathbf{a} = (a_1, \dots, a_p)'$ and $\mathbf{b} = (b_0, b_1, \dots, b_d)'$ satisfy

$$\begin{bmatrix} \mathbf{G} & \mathbf{E} \\ \mathbf{E}^T & \mathbf{0} \end{bmatrix} \begin{bmatrix} \mathbf{a} \\ \mathbf{b} \end{bmatrix} = \begin{bmatrix} \hat{\boldsymbol{\phi}}_k \\ \mathbf{0} \end{bmatrix}.$$

Here \mathbf{G} is a $p \times p$ matrix with the (i, j) -th element $g(\|\mathbf{s}_i - \mathbf{s}_j\|)$, and \mathbf{E} is a $p \times (d+1)$ matrix with the i -th row $(1, \mathbf{s}_i')$. Consequently, $\hat{\varphi}_k(\cdot)$ in (5) can be expressed in terms of $\hat{\boldsymbol{\phi}}_k$. Additionally, the roughness penalty can also be written as

$$J(\varphi_k) = \boldsymbol{\phi}'_k \boldsymbol{\Omega} \boldsymbol{\phi}_k, \quad (6)$$

with $\boldsymbol{\Omega}$ a known $p \times p$ matrix determined only by $\mathbf{s}_1, \dots, \mathbf{s}_p$. The readers are referred to [Green and Silverman \(1994\)](#) for more details regarding smoothing splines.

From (4) and (6), the proposed SpatPCA estimate of $\boldsymbol{\Phi}$ can be written as:

$$\hat{\boldsymbol{\Phi}}_{\tau_1, \tau_2} = \arg \min_{\boldsymbol{\Phi}: \boldsymbol{\Phi}'\boldsymbol{\Phi} = \mathbf{I}_K} \|\mathbf{Y} - \mathbf{Y}\boldsymbol{\Phi}\boldsymbol{\Phi}'\|_F^2 + \tau_1 \sum_{k=1}^K \boldsymbol{\phi}'_k \boldsymbol{\Omega} \boldsymbol{\phi}_k + \tau_2 \sum_{k=1}^K \sum_{j=1}^p |\phi_{jk}|, \quad (7)$$

subject to $\boldsymbol{\phi}'_1 \mathbf{S} \boldsymbol{\phi}_1 \geq \boldsymbol{\phi}'_2 \mathbf{S} \boldsymbol{\phi}_2 \geq \dots \geq \boldsymbol{\phi}'_K \mathbf{S} \boldsymbol{\phi}_K$. The resulting estimates of $\varphi_1(\cdot), \dots, \varphi_K(\cdot)$ can be directly computed from (5). When no confusion may arise, we shall simply write $\hat{\boldsymbol{\Phi}}_{\tau_1, \tau_2}$ as $\hat{\boldsymbol{\Phi}}$. Note that the SpatPCA estimate of (7) reduces to a sparse PCA estimate of [Zou, Hastie and Tibshirani \(2006\)](#) if the orthogonal constraint is dropped and $\boldsymbol{\Omega} = \mathbf{I}$ (i.e., no spatial structure is considered).

The tuning parameters τ_1 and τ_2 are selected using M -fold cross-validation (CV). First, we partition $\{1, \dots, n\}$ into M parts with as close to the same size as possible. Let $\mathbf{Y}^{(m)}$ be the sub-matrix of \mathbf{Y} corresponding to the m -th part, for $m = 1, \dots, M$. For each part, we treat $\mathbf{Y}^{(m)}$ as the validation data, and obtain the estimate $\hat{\boldsymbol{\Phi}}_{\tau_1, \tau_2}^{(-m)}$ of $\boldsymbol{\Phi}$ for $(\tau_1, \tau_2) \in \mathcal{A}$ based on the remaining data $\mathbf{Y}^{(-m)}$ using the proposed method, where $\mathcal{A} \subset [0, \infty)^2$ is a candidate index set. The proposed CV criterion is given in terms of an average residual sum of squares:

$$\text{CV}_1(\tau_1, \tau_2) = \frac{1}{M} \sum_{m=1}^M \|\mathbf{Y}^{(m)} - \mathbf{Y}^{(m)} \hat{\boldsymbol{\Phi}}_{\tau_1, \tau_2}^{(-m)} (\hat{\boldsymbol{\Phi}}_{\tau_1, \tau_2}^{(-m)})'\|_F^2, \quad (8)$$

where $\mathbf{Y}^{(m)} \hat{\boldsymbol{\Phi}}_{\tau_1, \tau_2}^{(-m)} (\hat{\boldsymbol{\Phi}}_{\tau_1, \tau_2}^{(-m)})'$ is the projection of $\mathbf{Y}^{(m)}$ onto the column space of $\hat{\boldsymbol{\Phi}}_{\tau_1, \tau_2}^{(-m)}$.

The final τ_1 and τ_2 values are $(\hat{\tau}_1, \hat{\tau}_2) = \arg \min_{(\tau_1, \tau_2) \in \mathcal{A}} \text{CV}_1(\tau_1, \tau_2)$.

2.2. Estimation of Spatial Covariance Function

To estimate $C_\eta(\cdot, \cdot)$ in (1), we also need to estimate the spatial covariance parameters, σ^2 and Λ . We apply the regularized least squares method of Tzeng and Huang (2015):

$$(\hat{\sigma}^2, \hat{\Lambda}) = \arg \min_{(\sigma^2, \Lambda): \sigma^2 \geq 0, \Lambda \succeq \mathbf{0}} \left\{ \frac{1}{2} \|\mathbf{S} - \hat{\Phi} \Lambda \hat{\Phi}' - \sigma^2 \mathbf{I}\|_F^2 + \gamma \|\hat{\Phi} \Lambda \hat{\Phi}'\|_* \right\}, \quad (9)$$

where $\gamma \geq 0$ is a tuning parameter, and $\|\mathbf{M}\|_* = \text{tr}((\mathbf{M}'\mathbf{M})^{1/2})$ is the nuclear norm of \mathbf{M} . The first term of (9) corresponds to goodness of fit by noting that $\text{var}(\mathbf{Y}_i) = \Phi \Lambda \Phi' + \sigma^2 \mathbf{I}$. The second term of (9) is a convex penalty, shrinking the eigenvalues of $\hat{\Phi} \Lambda \hat{\Phi}'$ to promote a low-rank structure and to avoid the eigenvalues being overestimated. By suitably choosing a tuning parameter γ , we can control the bias, while reducing the estimation variability. This is particularly effective when K is large.

Tzeng and Huang (2015) provides a closed-form solution for $\hat{\Lambda}$, but requires an iterative procedure for solving $\hat{\sigma}^2$. We found that closed-form expressions for both $\hat{\sigma}^2$ and $\hat{\Lambda}$ are available, and are shown in the following proposition with its proof given in the Appendix.

Proposition 1. *The solutions of (9) are given by*

$$\hat{\Lambda} = \hat{\mathbf{V}} \text{diag}(\hat{\lambda}_1^*, \dots, \hat{\lambda}_K^*) \hat{\mathbf{V}}', \quad (10)$$

$$\hat{\sigma}^2 = \begin{cases} \frac{1}{p - \hat{L}} \left(\text{tr}(\mathbf{S}) - \sum_{k=1}^{\hat{L}} (\hat{d}_k - \gamma) \right); & \text{if } \hat{d}_1 > \gamma, \\ \frac{1}{p} (\text{tr}(\mathbf{S})); & \text{if } \hat{d}_1 \leq \gamma, \end{cases} \quad (11)$$

where $\hat{\mathbf{V}} \text{diag}(\hat{d}_1, \dots, \hat{d}_K) \hat{\mathbf{V}}'$ is the eigen-decomposition of $\hat{\Phi}' \mathbf{S} \hat{\Phi}$ with $\hat{d}_1 \geq \dots \geq \hat{d}_K$,

$$\hat{L} = \max \left\{ L : \hat{d}_L - \gamma > \frac{1}{p - L} \left(\text{tr}(\mathbf{S}) - \sum_{k=1}^L (\hat{d}_k - \gamma) \right), L = 1, \dots, K \right\}, \quad (12)$$

and $\hat{\lambda}_k^* = \max(\hat{d}_k - \hat{\sigma}^2 - \gamma, 0)$; $k = 1, \dots, K$.

With $\hat{\Lambda} = (\hat{\lambda}_{kk'})_{K \times K}$ given by (9) and $\hat{\varphi}_k(\mathbf{s})$ given by (5), the proposed estimate of $C_\eta(\mathbf{s}, \mathbf{s}^*)$ is

$$\hat{C}_\eta(\mathbf{s}, \mathbf{s}^*) = \sum_{k=1}^K \sum_{k'=1}^K \hat{\lambda}_{kk'} \hat{\varphi}_k(\mathbf{s}) \hat{\varphi}_{k'}(\mathbf{s}^*). \quad (13)$$

Then the proposed estimate of $(\varphi_1^*(\mathbf{s}), \dots, \varphi_K^*(\mathbf{s}))$ is

$$(\hat{\varphi}_1^*(\mathbf{s}), \dots, \hat{\varphi}_K^*(\mathbf{s})) = (\hat{\varphi}_1(\mathbf{s}), \dots, \hat{\varphi}_K(\mathbf{s})) \hat{\mathbf{V}}; \quad \mathbf{s} \in D.$$

We consider M -fold CV to select γ . As in the previous section, we partition the data into M parts, $\mathbf{Y}^{(1)}, \dots, \mathbf{Y}^{(M)}$. For $m = 1, \dots, M$, we estimate $\text{var}(\mathbf{Y}^{(-m)})$ by $\hat{\Sigma}^{(-m)} = \hat{\Phi}^{(-m)} \hat{\Lambda}_\gamma^{(-m)} (\hat{\Phi}^{(-m)})' + (\hat{\sigma}_\gamma^2)^{(-m)} \mathbf{I}$ based on the remaining data $\mathbf{Y}^{(-m)}$ by removing $\mathbf{Y}^{(m)}$ from \mathbf{Y} , where $\hat{\Lambda}_\gamma^{(-m)}$, $(\hat{\sigma}_\gamma^2)^{(-m)}$ and $\hat{\Phi}^{(-m)}$ are the estimates of Λ , σ^2 and Φ based on $\mathbf{Y}^{(-m)}$, and for notational simplicity, their dependences on the selected (τ_1, τ_2) and K are suppressed. The proposed CV criterion is given by

$$\text{CV}_2(K, \gamma) = \frac{1}{M} \sum_{m=1}^M \|\mathbf{S}^{(m)} - \hat{\Phi}^{(-m)} \hat{\Lambda}_\gamma^{(-m)} (\hat{\Phi}^{(-m)})' - (\hat{\sigma}_\gamma^2)^{(-m)} \mathbf{I}\|_F^2, \quad (14)$$

where $\mathbf{S}^{(m)} = (\mathbf{Y}^{(m)})' \mathbf{Y}^{(m)} / n$. Then the γ selected by CV_2 based on K is $\hat{\gamma}_K = \arg \min_{\gamma \geq 0} \text{CV}_2(K, \gamma)$.

The dimension of eigen-space K , corresponding to the maximum rank of $\Phi \Lambda \Phi'$, could be selected by traditional approaches based on a given proportion of total variation explained or the scree plot of the sample eigenvalues. However, these approaches tend to be more subjective and may not be effective for the covariance estimation purpose. We propose to select K using CV_2 of (14) by subsequently increase the value of K from $K = 1, 2, \dots$, until no further reduction of the CV_2 value. Specifically, we select

$$\hat{K} = \min\{K : \text{CV}_2(K, \hat{\gamma}_K) \leq \text{CV}_2(K+1, \hat{\gamma}_{K+1}), K = 1, 2, \dots\}. \quad (15)$$

3. Computation Algorithm

Solving (7) is a challenging problem especially when both the orthogonal constraint and the L_1 penalty are involved simultaneously. Consequently, many regularized PCA

approaches, such as sparse PCA (Zou, Hastie and Tibshirani, 2006), do not cope with the orthogonal constraint. We adopt the ADMM algorithm by decomposing the original constrained optimization problem into small subproblems that can be efficiently handled through an iterative procedure. This type of algorithm was developed early in Gabay and Mercier (1976), and was systematically studied by Boyd et al. (2011) more recently.

First, the optimization problem of (7) is transferred into the following equivalent problem by adding an $p \times K$ parameter matrix \mathbf{Q} :

$$\min_{\Phi, \mathbf{Q} \in \mathbb{R}^{p \times K}} \|\mathbf{Y} - \mathbf{Y}\Phi\Phi'\|_F^2 + \tau_1 \sum_{k=1}^K \phi_k' \Omega \phi_k + \tau_2 \sum_{k=1}^K \sum_{j=1}^p |\phi_{jk}|, \quad (16)$$

subject to $\mathbf{Q}'\mathbf{Q} = \mathbf{I}_K$, $\phi_1' \mathbf{S} \phi_1 \geq \phi_2' \mathbf{S} \phi_2 \geq \dots \geq \phi_K' \mathbf{S} \phi_K$, and a new constrain, $\Phi = \mathbf{Q}$. Then the resulting constrained optimization problem of (16) is solved using the augmented Lagrangian method with its Lagrangian given by

$$\begin{aligned} L(\Phi, \mathbf{Q}, \Gamma) = & \|\mathbf{Y} - \mathbf{Y}\Phi\Phi'\|_F^2 + \tau_1 \sum_{k=1}^K \phi_k' \Omega \phi_k + \tau_2 \sum_{k=1}^K \sum_{j=1}^p |\phi_{jk}| \\ & + \text{tr}(\Gamma'(\Phi - \mathbf{Q})) + \frac{\rho}{2} \|\Phi - \mathbf{Q}\|_F^2, \end{aligned}$$

subject to $\mathbf{Q}'\mathbf{Q} = \mathbf{I}_K$ and $\phi_1' \mathbf{S} \phi_1 \geq \phi_2' \mathbf{S} \phi_2 \geq \dots \geq \phi_K' \mathbf{S} \phi_K$, where Γ is a $p \times K$ matrix of the Lagrange multipliers, and $\rho > 0$ is a penalty parameter to facilitate convergence. Note that the value of ρ does not affect the original optimization problem. The ADMM algorithm iteratively updates one group of parameters at a time in both the primal and the dual spaces until convergence. Given the initial estimates, $\mathbf{Q}^{(0)}$ and $\Gamma^{(0)}$ of \mathbf{Q} and Γ , our ADMM algorithm consists of the following steps at

the ℓ -th iteration:

$$\begin{aligned}\Phi^{(\ell+1)} &= \arg \min_{\Phi} L(\Phi, \mathbf{Q}^{(\ell)}, \Gamma^{(\ell)}) \\ &= \arg \min_{\Phi} \sum_{k=1}^K \left\{ \|\mathbf{z}_k^{(\ell)} - \mathbf{X}\phi_k\|^2 + \sum_{j=1}^p \tau_2 |\phi_{jk}| \right\},\end{aligned}\quad (17)$$

$$\mathbf{Q}^{(\ell+1)} = \arg \min_{\mathbf{Q}: \mathbf{Q}'\mathbf{Q}=\mathbf{I}_K} L(\Phi^{(\ell+1)}, \mathbf{Q}, \Gamma^{(\ell)}) = \mathbf{U}^{(\ell)}(\mathbf{V}^{(\ell)})', \quad (18)$$

$$\Gamma^{(\ell+1)} = \Gamma^{(\ell)} + \rho(\Phi^{(\ell+1)} - \mathbf{Q}^{(\ell+1)}), \quad (19)$$

where $\mathbf{X} = (\tau_1 \mathbf{\Omega} - \mathbf{Y}'\mathbf{Y} + \rho \mathbf{I}_p/2)^{1/2}$, $\mathbf{z}_k^{(\ell)}$ is the k -th column of $\mathbf{X}^{-1}(\rho \mathbf{Q}^{(\ell)} - \Gamma^{(\ell)})/2$, $\mathbf{U}^{(\ell)} \mathbf{D}^{(\ell)} (\mathbf{V}^{(\ell)})'$ is the singular value decomposition of $\Phi^{(\ell+1)} + \rho^{-1} \Gamma^{(\ell)}$, and ρ must be chosen large enough (e.g., twice the maximum eigenvalue of $\mathbf{Y}'\mathbf{Y}$) to ensure that \mathbf{X} is positive-definite. Note that (17) is simply a Lasso problem (Tibshirani (1996)), which can be solved effectively using the coordinate descent algorithm (Friedman, Hastie and Tibshirani, 2010).

Except (17), the ADMM steps given by (17)-(19) have closed-form expressions. In fact, we can make the algorithm involve only closed-form updates by further decomposing (17) into another ADMM step. Specifically, we can introduce another parameters r_{jk} 's to replace the last term of (16) and add the constraint, $\phi_{jk} = r_{jk}$ for $j = 1, \dots, p$ and $k = 1, \dots, K$, to form an equivalent problem:

$$\min_{\Phi, \mathbf{Q}, \mathbf{R}} \|\mathbf{Y} - \mathbf{Y}\Phi\Phi'\|_F^2 + \tau_1 \sum_{k=1}^K \phi'_i \mathbf{\Omega} \phi_k + \tau_2 \sum_{k=1}^K \sum_{j=1}^p |r_{jk}|,$$

subject to $\mathbf{Q}'\mathbf{Q} = \mathbf{I}_K$, $\Phi = \mathbf{Q} = \mathbf{R}$, and $\phi'_1 \mathbf{S} \phi_1 \geq \phi'_2 \mathbf{S} \phi_2 \geq \dots \geq \phi'_K \mathbf{S} \phi_K$, where r_{jk} is the (j, k) -th element of \mathbf{R} . Then the corresponding augmented Lagrangian is

$$\begin{aligned}L(\Phi, \mathbf{Q}, \mathbf{R}, \Gamma_1, \Gamma_2) &= \|\mathbf{Y} - \mathbf{Y}\Phi\Phi'\|_F^2 + \tau_1 \sum_{k=1}^K \phi'_i \mathbf{\Omega} \phi_k + \tau_2 \sum_{k=1}^K \sum_{j=1}^p |r_{jk}| \\ &\quad + \text{tr}(\Gamma_1'(\Phi - \mathbf{Q})) + \text{tr}(\Gamma_2'(\Phi - \mathbf{R})) \\ &\quad + \frac{\rho}{2} (\|\Phi - \mathbf{Q}\|_F^2 + \|\Phi - \mathbf{R}\|_F^2),\end{aligned}$$

subject to $\mathbf{Q}'\mathbf{Q} = \mathbf{I}_K$ and $\phi'_1 \mathbf{S} \phi_1 \geq \phi'_2 \mathbf{S} \phi_2 \geq \dots \geq \phi'_K \mathbf{S} \phi_K$, where Γ_1 and Γ_2 are $p \times K$ matrices of the Lagrange multipliers. Then the ADMM steps at the ℓ -th

iteration are given by

$$\begin{aligned}\Phi^{(\ell+1)} &= \arg \min_{\Phi} L(\Phi, \mathbf{Q}^{(\ell)}, \mathbf{R}^{(\ell)}, \Gamma_1^{(\ell)}, \Gamma_2^{(\ell)}) \\ &= \frac{1}{2}(\tau_1 \Omega + \rho \mathbf{I}_p - \mathbf{Y}'\mathbf{Y})^{-1} \{ \rho(\mathbf{Q}^{(\ell)} + \mathbf{R}^{(\ell)}) - \Gamma_1 - \Gamma_2 \},\end{aligned}\quad (20)$$

$$\mathbf{Q}^{(\ell+1)} = \arg \min_{\mathbf{Q}: \mathbf{Q}'\mathbf{Q}=\mathbf{I}_K} L(\Phi^{(\ell+1)}, \mathbf{Q}, \mathbf{R}^{(\ell)}, \Gamma_1^{(\ell)}, \Gamma_2^{(\ell)}) = \mathbf{U}^{(\ell)} (\mathbf{V}^{(\ell)})', \quad (21)$$

$$\begin{aligned}\mathbf{R}^{(\ell+1)} &= \arg \min_{\mathbf{R}} L(\Phi^{(\ell+1)}, \mathbf{Q}^{(\ell+1)}, \mathbf{R}, \Gamma_1^{(\ell)}, \Gamma_2^{(\ell)}) \\ &= \frac{1}{\rho} \mathcal{S}_{\tau_2}(\rho \Phi^{(\ell+1)} + \Gamma_2^{(\ell)}),\end{aligned}\quad (22)$$

$$\Gamma_1^{(\ell+1)} = \Gamma_1^{(\ell)} + \rho (\Phi^{(\ell+1)} - \mathbf{Q}^{(\ell+1)}), \quad (23)$$

$$\Gamma_2^{(\ell+1)} = \Gamma_2^{(\ell)} + \rho (\Phi^{(\ell+1)} - \mathbf{R}^{(\ell+1)}), \quad (24)$$

where $\mathbf{R}^{(0)}$, $\Gamma_1^{(0)}$ and $\Gamma_2^{(0)}$ are initial estimates of \mathbf{R} , Γ_1 and Γ_2 , respectively, $\mathbf{U}^{(\ell)} \mathbf{D}^{(\ell)} (\mathbf{V}^{(\ell)})'$ is the singular value decomposition of $\Phi^{(\ell+1)} + \rho^{-1} \Gamma_1^{(\ell)}$, and $\mathcal{S}_{\tau_2}(\cdot)$ is the element-wise soft-thresholding operator with a threshold τ_2 (i.e., the (j, k) -th element of $\mathcal{S}_{\tau_2}(\mathbf{M})$ is $\text{sign}(m_{jk}) \max(|m_{jk}| - \tau_2, 0)$ with m_{jk} the (j, k) -th element of \mathbf{M}). Similarly to (17), ρ must be chosen large enough to ensure that $\tau_1 \Omega + \rho \mathbf{I}_p - \mathbf{Y}'\mathbf{Y}$ in (20) is positive definite.

4. Numerical Examples

We conducted some simulation experiments in one-dimensional and two-dimensional spatial domains, and applied SpatPCA to a real-world dataset. We compared the proposed SpatPCA with three methods: (1) PCA ($\tau_1 = \tau_2 = 0$); (2) SpatPCA with the smoothness penalty only ($\tau_2 = 0$); (3) SpatPCA with the sparseness penalty only ($\tau_1 = 0$), based on the two loss functions. The first one measures the prediction ability in terms of an average squared prediction error:

$$\text{Loss}(\hat{\Phi}) = \frac{1}{n} \sum_{i=1}^n \|\hat{\Phi} \hat{\xi}_i - \Phi \xi_i\|^2, \quad (25)$$

where Φ is the true eigenvector matrix formed by the first K eigenvectors and

$$\hat{\xi}_i = \hat{\mathbf{V}} \text{diag} \left(\frac{\hat{\lambda}_1^*}{\hat{\lambda}_1^* + \hat{\sigma}^2}, \dots, \frac{\hat{\lambda}_K^*}{\hat{\lambda}_K^* + \hat{\sigma}^2} \right) \hat{\mathbf{V}}' \hat{\Phi}' \mathbf{Y}_i,$$

is the empirical best linear unbiased predictor of $\boldsymbol{\xi}_i$ with the estimated parameters plugged in. The second one concerns the goodness of covariance function estimation in terms of an average squared estimation error:

$$\text{Loss}(\hat{C}_\eta) = \frac{1}{p^2} \sum_{i=1}^p \sum_{j=1}^p (\hat{C}_\eta(\mathbf{s}_i, \mathbf{s}_j) - C_\eta(\mathbf{s}_i, \mathbf{s}_j))^2. \quad (26)$$

We applied the ADMM algorithm given by (20)-(24) to compute the SpatPCA estimates with ρ being ten times the maximum eigenvalue of $\mathbf{Y}'\mathbf{Y}$. The stopping criterion for the ADMM algorithm is

$$\frac{1}{\sqrt{p}} \max (\|\boldsymbol{\Phi}^{(\ell+1)} - \boldsymbol{\Phi}^{(\ell)}\|_F, \|\boldsymbol{\Phi}^{(\ell+1)} - \mathbf{R}^{(\ell+1)}\|_F, \|\boldsymbol{\Phi}^{(\ell+1)} - \mathbf{Q}^{(\ell+1)}\|_F) \leq 10^{-4}.$$

4.1. One-Dimensional Experiment

In the first experiment, we generated data according to (3) with $K = 2$, $\boldsymbol{\xi}_i \sim N(\mathbf{0}, \text{diag}(\lambda_1, \lambda_2))$, $\boldsymbol{\epsilon}_i \sim N(\mathbf{0}, \mathbf{I})$, $n = 100$, $p = 50$, $\mathbf{s}_1, \dots, \mathbf{s}_{50}$ equally spaced in $D = [-5, 5]$, and

$$\phi_1(\mathbf{s}) = \frac{1}{c_1} \exp(-(x_1^2 + \dots + x_d^2)), \quad (27)$$

$$\phi_2(\mathbf{s}) = \frac{1}{c_2} x_1 \cdots x_d \exp(-(x_1^2 + \dots + x_d^2)), \quad (28)$$

where $\mathbf{s} = (x_1, \dots, x_d)'$, c_1 and c_2 are normalization constants such that $\|\phi_1\|_2 = \|\phi_2\|_2 = 1$, and $d = 1$. We considered three pairs of $(\lambda_1, \lambda_2) \in \{(9, 0), (1, 0), (9, 4)\}$, and applied the proposed SpatPCA with $K \in \{1, 2, 5\}$ and \hat{K} selected from (15), resulting in 12 different combinations. For each combination, we considered 11 values of τ_1 (including 0, and the other 10 values from 1 to 10^3 equally spaced on the log scale) and 31 values of τ_2 (including 0, and the other 30 values from 1 to 10^3 equally spaced on the log scale). But instead of performing a two-dimensional optimization by selecting among all possible pairs of (τ_1, τ_2) , we applied a more efficient two-step procedure involving only one-dimensional optimization. First, we selected among 11 values of τ_1 by fixing $\tau_2 = 0$ using 5-fold CV of (8) with the initial estimate of $\hat{\boldsymbol{\Phi}}_{\tau_1, 0}^{(0)}$

given by the first K eigenvectors of $\mathbf{Y}'\mathbf{Y} - \tau_1\mathbf{\Omega}$ as its columns. Note that this initial estimate is actually the true estimate $\hat{\mathbf{\Phi}}_{\tau_1,0}$ when $\mathbf{Y}'\mathbf{Y} - \tau_1\mathbf{\Omega} \succeq \mathbf{0}$. Then we selected among 31 values of τ_2 with the selected τ_1 using 5-fold CV of (8).

For covariance function estimation, we selected the tuning parameter γ among 11 values of γ using 5-fold CV of (14), including $\gamma = 0$ and the other 10 values from 1 to \hat{d}_1 equally spaced on the log scale, where \hat{d}_1 is the largest eigenvalues of $\hat{\mathbf{\Phi}}'\mathbf{S}\hat{\mathbf{\Phi}}$.

Figure 1 shows the estimates of $\phi_1(\cdot)$ and $\phi_2(\cdot)$ for the four methods based on three different combinations of eigenvalues. Each case contains two estimated functions based on two randomly generated datasets. As expected, the PCA estimates, which consider no spatial structure, are very noisy, particularly when the signal-to-noise ratio is small. Adding only the smoothness penalty (i.e., $\tau_2 = 0$) makes the estimates considerably less noisy. But the resulting estimates show some obvious bias. On the other hand, adding only the sparseness penalty (i.e., $\tau_1 = 0$) forces the eigenfunction estimates to be zeros at some locations. But the estimated patterns are still very noisy. Overall, our SpatPCA estimates reproduce the targets with little noise for all cases even when the signal-to-noise ratio is small, indicating the effectiveness of regularization.

Figure 2 shows the covariance function estimates for the four methods based on a randomly generated dataset. The proposed SpatPCA can be seen to perform considerably better than the other methods for all cases by being able to reconstruct the underlying nonstationary spatial covariance functions without having noticeable visual artifacts.

The performance of the four methods in terms of the loss functions (25) and (26) is shown in Figures 3 and 4, respectively, based on 50 simulation replicates. Once again, SpatPCA outperforms all the other methods in all cases. For $(\lambda_1, \lambda_2) = (9, 0)$, the average computation time for SpatPCA (including selection of λ_1 and λ_2 using 5-fold CV) with $K = 1, 2, 5$ are 0.020, 0.065 and 0.264 seconds, respectively, which are larger than 0.002 seconds required for PCA. The results were conducted using our

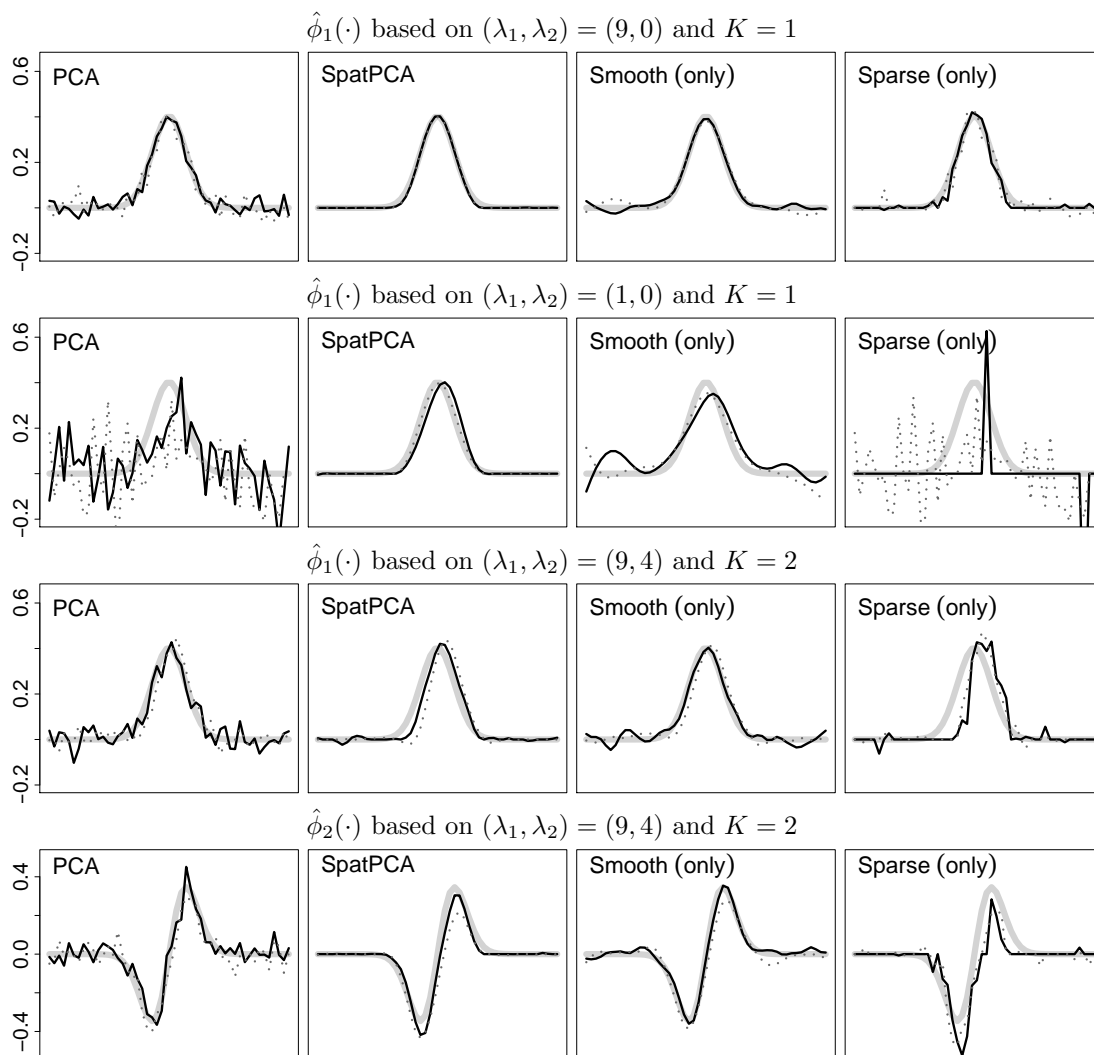


FIG 1. Estimates of $\phi_1(\cdot)$ and $\phi_2(\cdot)$ obtained from various methods based on three different combinations of eigenvalues. Each panel consists of two estimates (in two different line types) corresponding to two randomly generated datasets, where the solid grey lines are the true eigenfunctions.

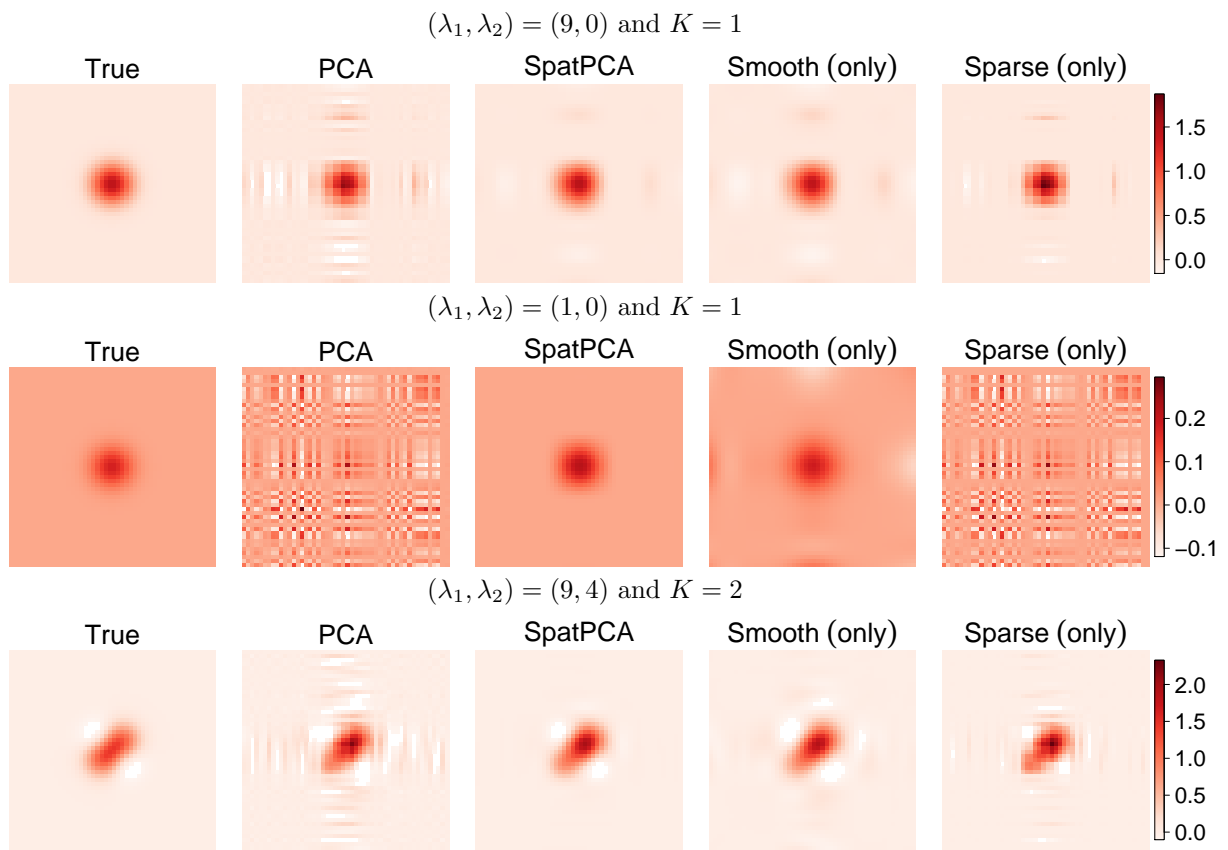


FIG 2. True covariance functions and their estimates obtained from various methods based on three different combinations of eigenvalues.

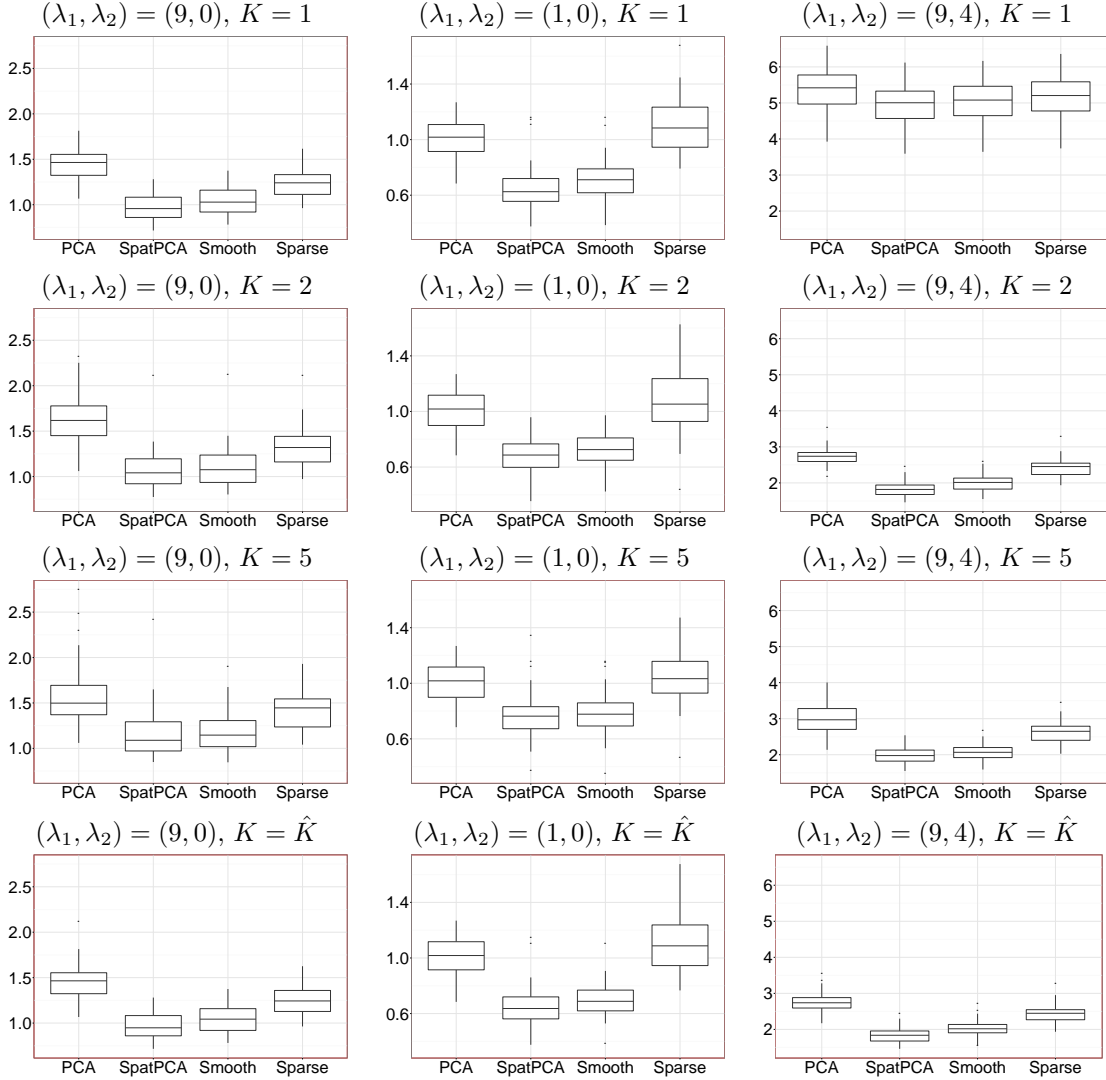


FIG 3. Boxplots of average squared prediction errors of (25) for various methods in the one-dimensional simulation experiment of Section 4.1 based on 50 simulation replicates.

R package “SpatPCA” implemented on an iMac PC equipped with a 3.2GHz Intel Core i5 CPU and a 64GB RAM.

4.2. Two-Dimensional Experiment I

We considered a two-dimensional experiment by generating data according to (3) with $K = 2$, $\xi_i \sim N(\mathbf{0}, \text{diag}(\lambda_1, \lambda_2))$, $\epsilon_i \sim N(\mathbf{0}, \mathbf{I})$, $n = 500$, $\mathbf{s}_1, \dots, \mathbf{s}_p$ regularly spaced at $p = 20^2$ locations in $D = [-5, 5]^2$. Here $\phi_1(\cdot)$ and $\phi_2(\cdot)$ are given by (27) and (28) with $d = 2$ (see the images in the first column of Figure 5).

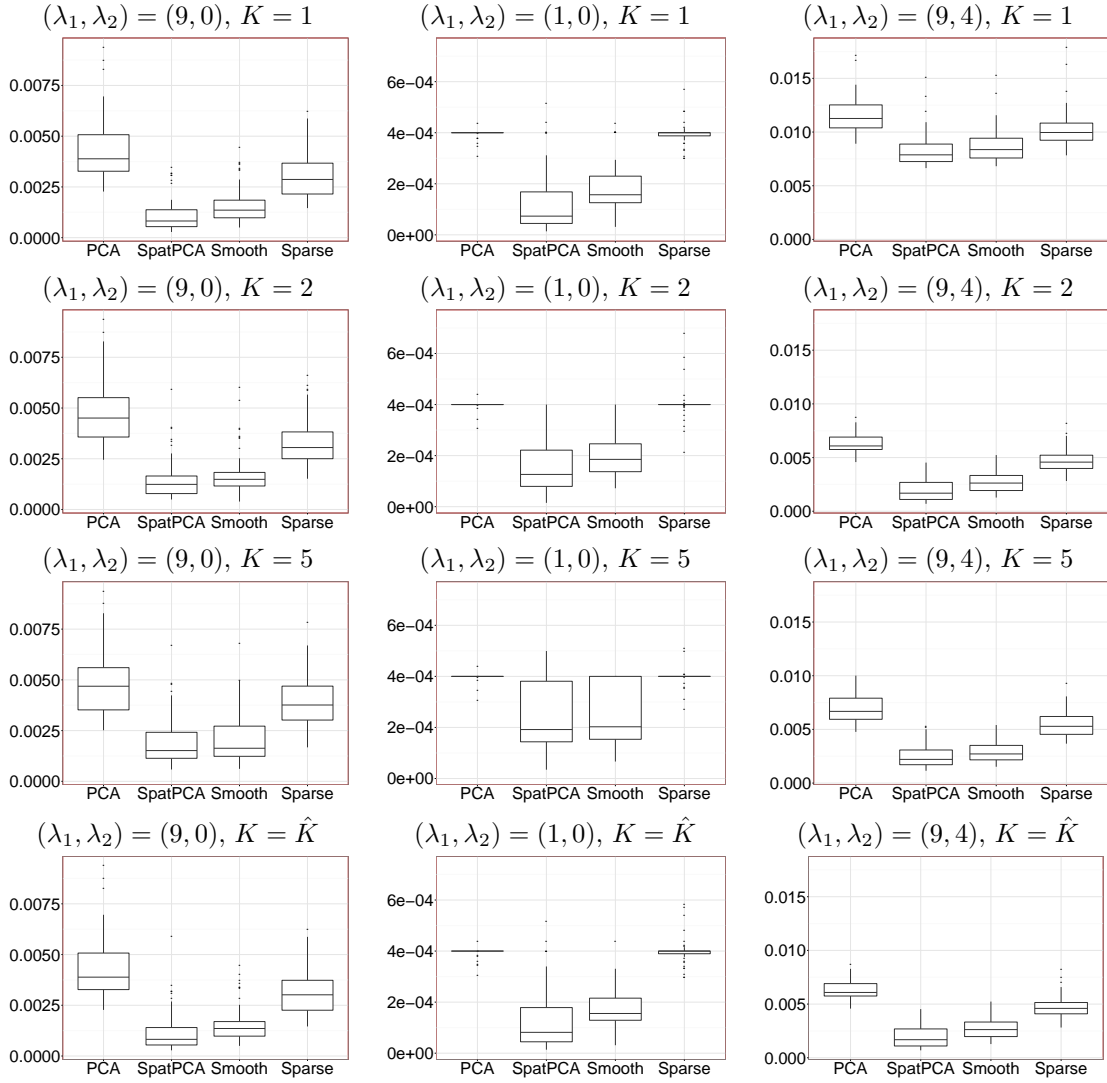


FIG 4. Boxplots of average squared estimation errors of (26) for various methods in the one-dimensional simulation experiment of Section 4.1 based on 50 simulation replicates.

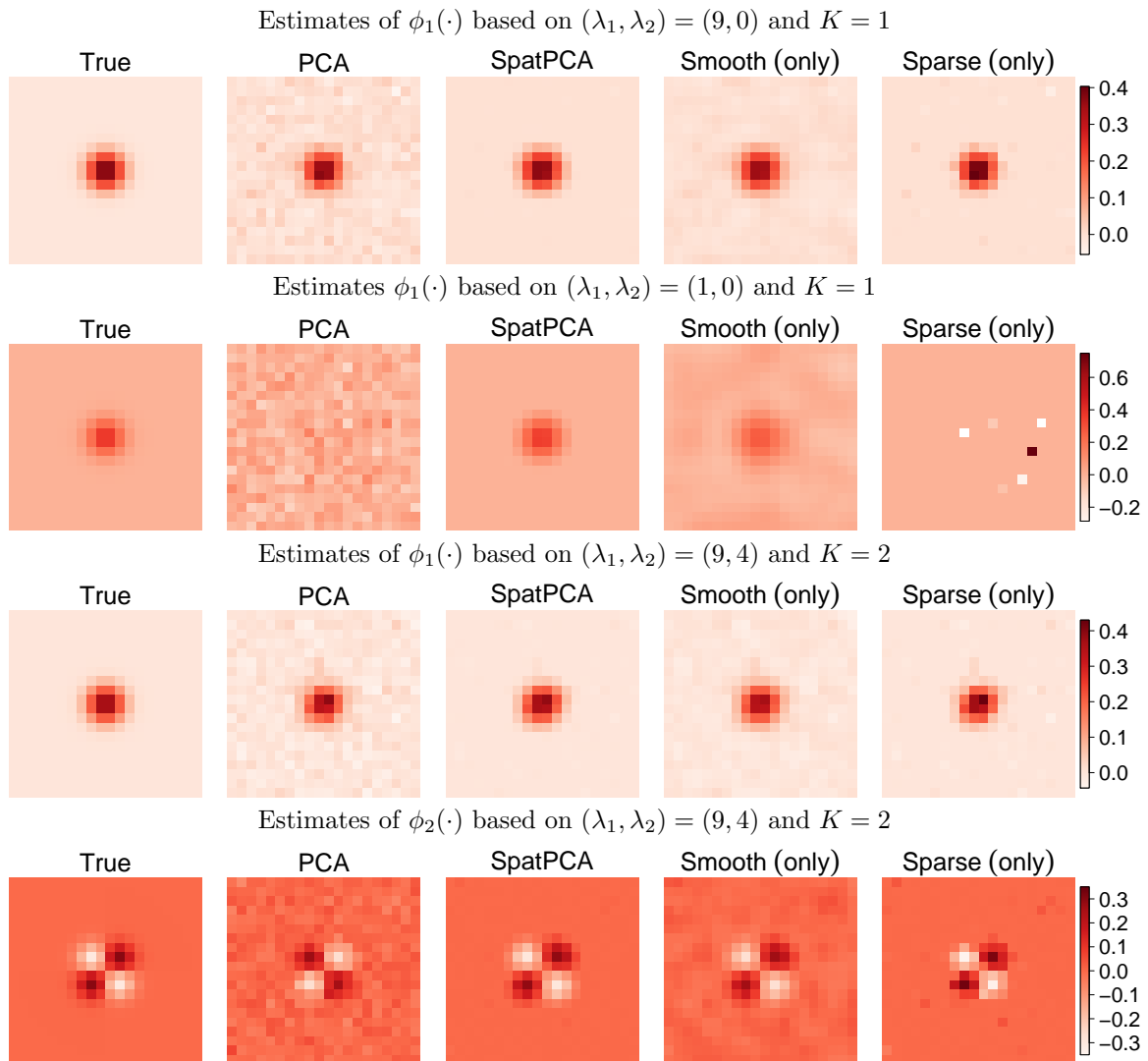


FIG 5. Estimates of $\phi_1(\cdot)$ and $\phi_2(\cdot)$ obtained from various methods based on three different combinations of eigenvalues.

We considered three pairs of $(\lambda_1, \lambda_2) \in \{(9, 0), (1, 0), (9, 4)\}$, and applied the proposed SpatPCA with $K \in \{1, 2, 5\}$ and \hat{K} selected from (15). As in the one-dimensional experiment, we used 5-fold CV of (8) and a two-step procedure to select among the same 11 values of τ_1 and 31 values of τ_2 . Similarly, we used 5-fold CV of (14) to select among the same 11 values of γ for covariance function estimation.

Figure 5 shows the estimates of $\phi_1(\cdot)$ and $\phi_2(\cdot)$ obtained from the four methods for various cases based on a randomly generated dataset. The performance of the four methods in terms of the loss functions (25) and (26) is summarized in Figure 6 and Figure 7, respectively, based on 50 simulation replicates. Similarly to the one-dimensional examples, SpatPCA performs significantly better than all the other methods in all cases. For $(\lambda_1, \lambda_2) = (9, 0)$, the average computation time for SpatPCA (including selection of λ_1 and λ_2 using 5-fold CV) with $K = 1, 2, 5$ are 3.105, 4.242 and 16.160 seconds, respectively, using the R package ‘‘SpatPCA’’ implemented on an iMac PC with a 3.2GHz Intel Core i5 CPU and a 64GB RAM. While SpatPCA is slower than PCA (requiring only 0.267 seconds), it is reasonably fast and provides much improved results.

4.3. An Application to a Sea Surface Temperature Dataset

Since the proposed SpatPCA works better when both smoothness and sparseness penalties are involved according to the simulation experiments in Sections 4.1 and 4.2, we applied the proposed SpatPCA with both penalty terms to a sea surface temperature (SST) dataset observed over a region in the Indian Ocean, and only compared it with PCA. The data are monthly averages of SST obtained from the Met Office Marine Data Bank (available at <http://www.metoffice.gov.uk/hadobs/hadisst/>) on 1 degree latitude by 1 degree longitude ($1^\circ \times 1^\circ$) equiangular grid cells from January 2001 to December 2010 in the region between latitudes $20^\circ N$ and $20^\circ S$ and between longitudes $39^\circ E$ and $120^\circ E$. Out of $40 \times 81 = 3,240$ grid cells, there are 460 cells on the land where no data are available. Hence the data we used are

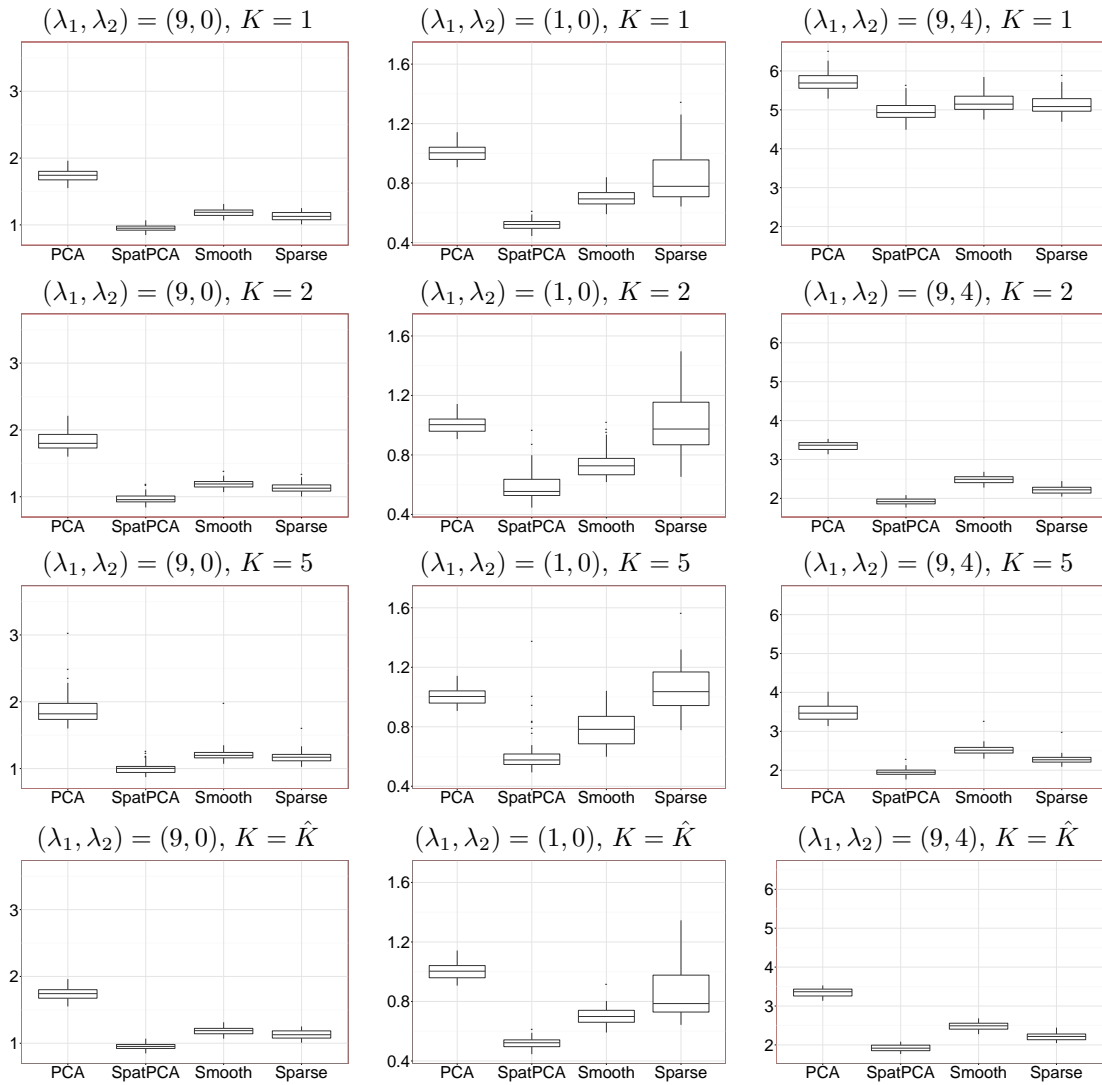


FIG 6. Boxplots of average squared prediction errors of (25) for various methods in the two-dimensional simulation experiment of Section 4.2 based on 50 simulation replicates.

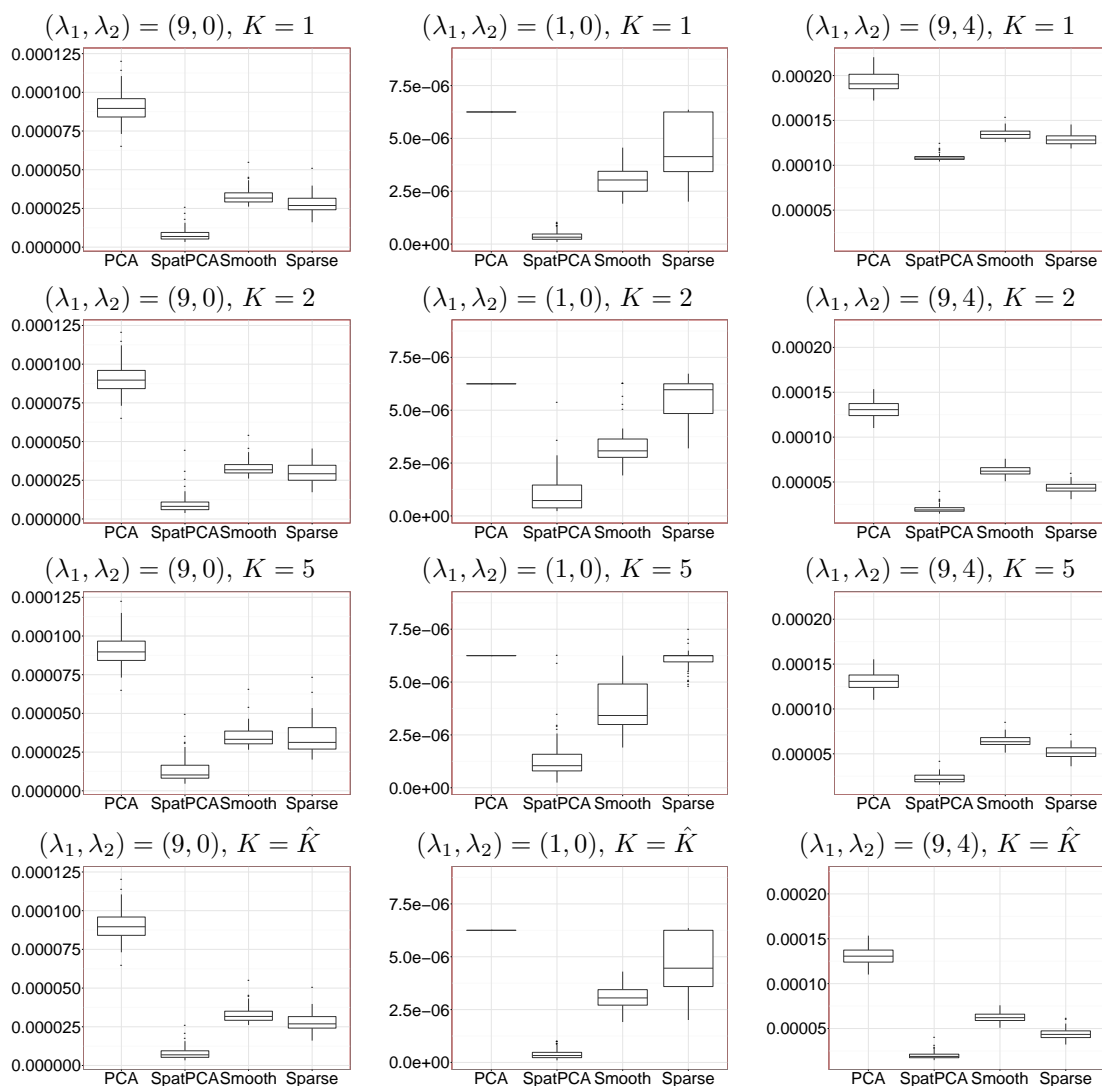


FIG 7. Boxplots of average squared estimation errors of (26) for various methods in the two-dimensional simulation experiment of Section 4.2 based on 50 simulation replicates.

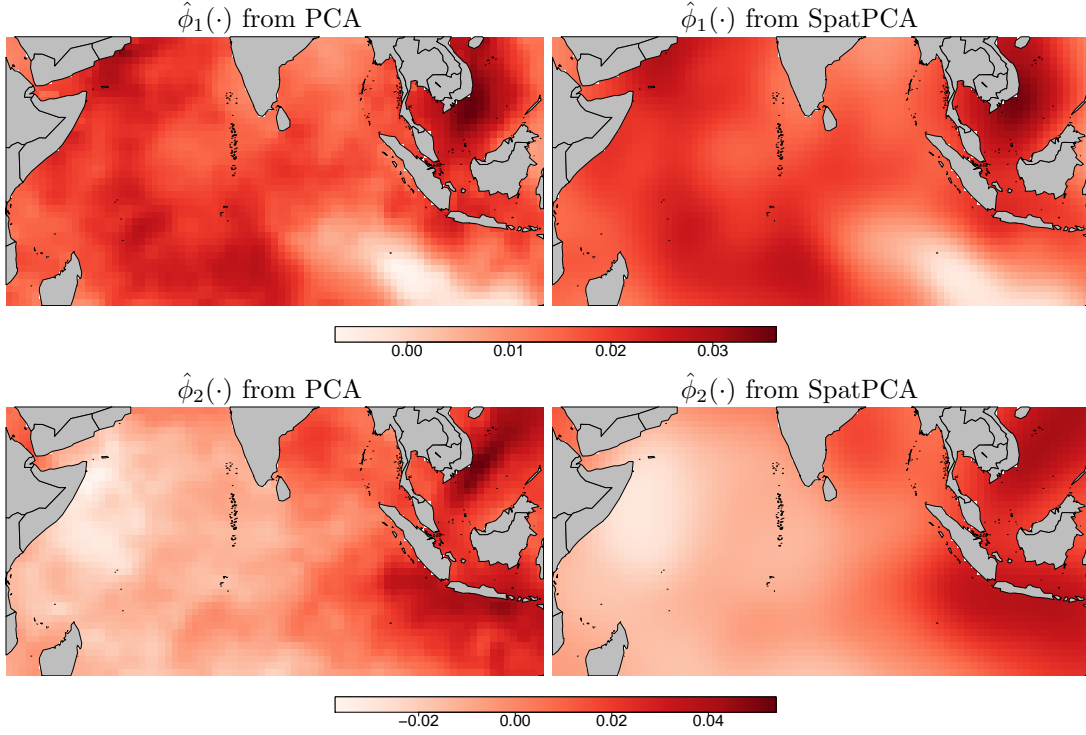


FIG 8. *Estimated eigenimages obtained from PCA and SpatPCA over a region in the Indian Ocean, where the gray regions correspond to the land.*

observed at $p = 2,780$ cells and 120 time points. We first detrended the SST data by subtracting the SST for a given cell and a given month by the average SST for that cell and that month over the whole period. We decomposed the data into two parts with one part consisting of 60 time points of $\{1, 3, \dots, 119\}$ for training data, and the other part, consisting of 60 time points of even numbers, for validation purpose.

We applied SpatPCA on the training data with K selected by \hat{K} of (15). Similar to the two-step method described in Section 4.1, we selected among 11 values of τ_1 (including 0, and the other 10 values from 10^3 to 10^8 equally spaced on the log scale) and 31 values of τ_2 (including 0, and the other 30 values from 1 to 10^3 equally spaced on the log scale) using 5-fold CV of (8). For both PCA and SpatPCA, we applied 5-fold CV of (14) to select among 11 values of γ (including 0 and other 10 values from $\hat{d}_1/10^3$ to \hat{d}_1 equally spaced on the log scale), where \hat{d}_1 is the largest eigenvalue of $\hat{\Phi}'\mathbf{S}\hat{\Phi}$.

The first two dominant patterns estimated from PCA and SpatPCA are shown

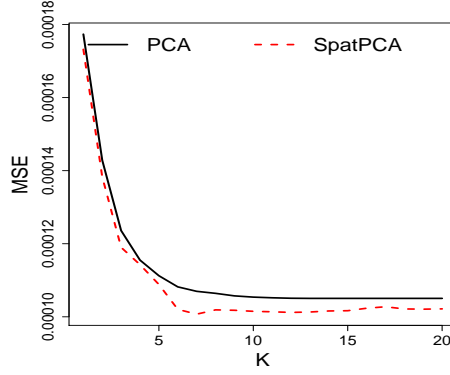


FIG 9. Mean squared errors of covariance matrix estimation with respect to K for PCA and SpatPCA.

in Figure 8. Both methods identify similar patterns with the ones estimated from SpatPCA being a bit smoother than those estimated from PCA. The first pattern is a basin-wide mode and the second one corresponds to the east-west dipole mode (Deser et al. (2009)).

We used the validation data to evaluate the performance between PCA and SpatPCA in terms of the mean squared error (MSE), $\|\hat{\Sigma} - \mathbf{S}_v\|_F^2/p^2$, where $\hat{\Sigma}$ is a generic estimate of $\text{var}(\mathbf{Y})$ based on the training data, and \mathbf{S}_v is the sample covariance matrix based on the validation data. The resulting MSE for PCA is 1.05×10^{-4} , which is slightly larger than 1.02×10^{-4} for SpatPCA. Figure 9 shows the MSEs with respect to various K values for both PCA and SpatPCA. The results indicate that SpatPCA is not sensitive to the choice of K as long as K is sufficiently large. Our choice of $\hat{K} = 6$ for SpatPCA based on (15) appears to be effective, and is smaller than $\hat{K} = 15$ for PCA.

4.4. Two-Dimensional Experiment II

To reflect a real-world situation, we generated data by mimicking the SST dataset analyzed in the previous subsection, except we applied a larger noise variance. Specifically, we generated data according to (3) with $K = 2$, $\boldsymbol{\xi}_i \sim N(\mathbf{0}, \text{diag}(\lambda_1, \lambda_2))$, $\boldsymbol{\epsilon}_i \sim N(\mathbf{0}, \mathbf{I})$, $n = 60$, and at the same 2,780 locations from the SST dataset. Here $\phi_1(\cdot)$ and $\phi_2(\cdot)$ are given by $\hat{\phi}_1(\cdot)$ and $\hat{\phi}_2(\cdot)$ (see Figure 8) and $(\lambda_1, \lambda_2) = (91.3, 16.1)$

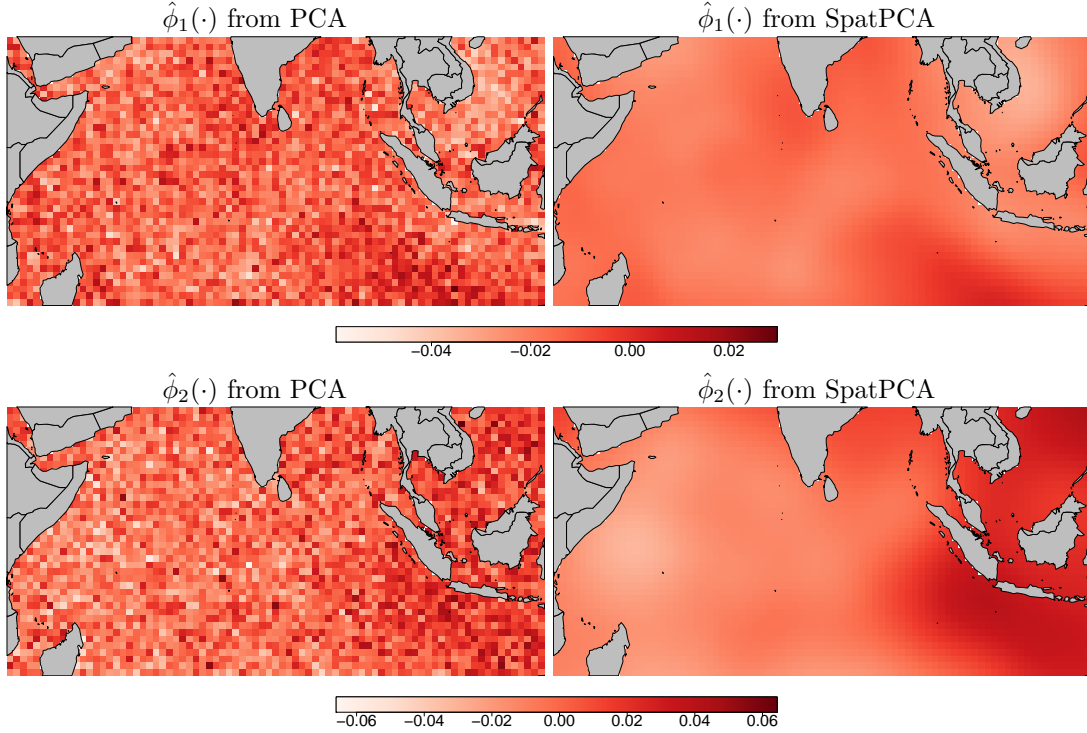


FIG 10. Estimates of $\phi_1(\cdot)$ and $\phi_2(\cdot)$ obtained from PCA and SpatPCA in the two-dimensional experiment of Section 4.4 based on a randomly simulated dataset, where the areas in gray are the land.

estimated by SpatPCA in the previous subsection.

We applied the 5-fold CV of (14) and (15) to select the tuning parameters (τ_1, τ_2) and K in the same way as in the previous subsection. Figure 10 shows the estimates of $\phi_1(\cdot)$ and $\phi_2(\cdot)$ for PCA and SpatPCA based on a randomly generated dataset. Because we consider a larger noise variance than those in the previous subsection, the first two patterns estimated from PCA turn out to be very noisy. In contrast, SpatPCA can still reconstruct the first two patterns very well with little noise. The results in terms of the loss functions of (25) and (26) are summarized in Figure 11. Once again, SpatPCA outperforms PCA by a large margin.

Acknowledgements

The authors are grateful to the associate editor and the two referees for their insightful and constructive comments, which greatly improve the presentation of this paper. This

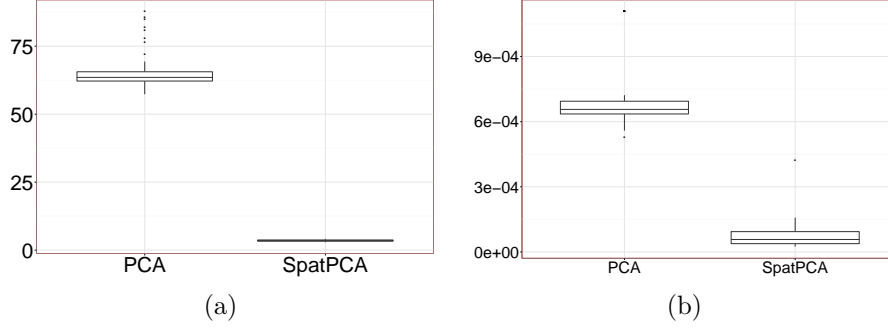


FIG 11. (a) Boxplots of loss function values for PCA and SpatPCA in the two-dimensional simulation experiment of Section 4.4 based on 50 simulation replicates: (a) Average squared prediction errors of (25); (b) Average squared estimation errors of (26).

research was supported in part by ROC Ministry of Science and Technology grant MOST 103-2118-M-001-007-MY3.

Appendix

Proof of Proposition 1. First, we prove (10). From Corollary 1 of Tzeng and Huang (2015), the minimizer of $h(\Lambda, \sigma^2)$ given σ^2 is

$$\hat{\Lambda}(\sigma^2) = \hat{\mathbf{V}} \text{diag}((\hat{d}_1 - \sigma^2 - \gamma)_+, \dots, (\hat{d}_K - \sigma^2 - \gamma)_+) \hat{\mathbf{V}}'. \quad (29)$$

Hence (10) is obtained.

Next, we prove (11). Rewrite the objective function of (9) as:

$$\begin{aligned} h(\Lambda, \sigma^2) &= \frac{1}{2} \|\hat{\Phi} \hat{\Phi}' \mathbf{S} \hat{\Phi} \hat{\Phi}' - \hat{\Phi} \Lambda \hat{\Phi}' - \sigma^2 \mathbf{I}_p\|_F^2 + \frac{1}{2} \|\mathbf{S} - \hat{\Phi} \hat{\Phi}' \mathbf{S} \hat{\Phi} \hat{\Phi}'\|_F^2 \\ &\quad + \sigma^2 \text{tr}(\hat{\Phi} \hat{\Phi}' \mathbf{S} \hat{\Phi} \hat{\Phi}' - \mathbf{S}) + \gamma \|\hat{\Phi} \Lambda \hat{\Phi}'\|_*. \end{aligned} \quad (30)$$

From (29) and (30), we have

$$\begin{aligned} h(\hat{\Lambda}(\sigma^2), \sigma^2) &= \frac{1}{2} \|\hat{\Phi} \hat{\Phi}' \mathbf{S} \hat{\Phi} \hat{\Phi}' - \hat{\Phi} \hat{\Lambda}(\sigma^2) \hat{\Phi}' - \sigma^2 \mathbf{I}_p\|_F^2 + \gamma \|\hat{\Phi} \hat{\Lambda}(\sigma^2) \hat{\Phi}'\|_* \\ &\quad + \frac{1}{2} \|\mathbf{S} - \hat{\Phi} \hat{\Phi}' \mathbf{S} \hat{\Phi} \hat{\Phi}'\|_F^2 + \sigma^2 \text{tr}(\hat{\Phi} \hat{\Phi}' \mathbf{S} \hat{\Phi} \hat{\Phi}' - \mathbf{S}) \\ &= \frac{1}{2} \sum_{k=1}^K \{ \hat{d}_k^2 - (\hat{d}_k - \sigma^2 - \gamma)_+^2 \} + \frac{p}{2} \sigma^4 - \sigma^2 \text{tr}(\mathbf{S}) + \frac{1}{2} \|\mathbf{S} - \hat{\Phi} \hat{\Phi}' \mathbf{S} \hat{\Phi} \hat{\Phi}'\|_F^2. \end{aligned}$$

Minimizing $h(\hat{\mathbf{\Lambda}}(\sigma^2), \sigma^2)$, we obtain

$$\hat{\sigma}^2 = \arg \min_{\sigma^2 \geq 0} \left\{ p\sigma^4 - 2\sigma^2 \text{tr}(\mathbf{S}) - \sum_{k=1}^K (\hat{d}_k - \sigma^2 - \gamma)_+^2 \right\}. \quad (31)$$

Clearly, if $\hat{d}_1 \leq \gamma$, then $\hat{\sigma}^2 = \frac{1}{p} \text{tr}(\mathbf{S})$. We remain to consider $\hat{d}_1 > \gamma$. Let

$$\hat{L}^* = \max \{L : \hat{d}_L - \gamma > \hat{\sigma}^2, L = 1, \dots, K\}.$$

From (31), $\hat{\sigma}^2 = \frac{1}{p - \hat{L}^*} \left(\text{tr}(\mathbf{S}) - \sum_{k=1}^{\hat{L}^*} (\hat{d}_k - \gamma) \right)$. It suffices to show that $\hat{L}^* = \hat{L}$. Since

$\hat{d}_{\hat{L}^*} - \gamma > \frac{1}{p - \hat{L}^*} \left(\text{tr}(\mathbf{S}) - \sum_{k=1}^{\hat{L}^*} (\hat{d}_k - \gamma) \right)$, by the definition of \hat{L} , we have $\hat{L} \geq \hat{L}^*$,

implying $\hat{d}_{\hat{L}} \geq \hat{d}_{\hat{L}^*}$. Suppose that $\hat{L} > \hat{L}^*$. It immediately follows from the definition of \hat{L}^* that $\hat{d}_{\hat{L}} - \gamma \leq \hat{\sigma}^2 < \hat{d}_{\hat{L}^*} - \gamma$, which contradicts to $\hat{d}_{\hat{L}} \geq \hat{d}_{\hat{L}^*}$. Therefore, $\hat{L} = \hat{L}^*$.

This completes the proof. \square

References

- BOYD, S., PARIKH, N., CHU, E., PELEATO, B. and ECKSTEIN, J. (2011). Distributed optimization and statistical learning via the alternating direction method of multipliers. *Foundations and Trends in Machine Learning* **3** 1-124.
- CRESSIE, N. and JOHANNESSON, G. (2008). Fixed Rank Kriging for Very Large Spatial Data Sets. *Journal of the Royal Statistical Society. Series B* **70** 209-226.
- D'ASPREMONT, A., BACH, F. and GHAOUI, L. E. (2008). Optimal solutions for sparse principal component analysis. *Journal of Machine Learning Research* **9** 1269-1294.
- DEMSAR, U., HARRIS, P., BRUNSDON, C., FOTHERINGHAM, A. S. and MCLOONE, S. (2013). Principal component analysis on spatial data: an overview. *Annals of the Association of American Geographers* **103** 106-128.
- DESER, C., ALEXANDER, M. A., XIE, S.-P. and PHILLIPS, A. S. (2009). Sea surface temperature variability: patterns and mechanisms. *Annual Review of Marine Science* **2** 115-143.

- FRIEDMAN, J., HASTIE, T. and TIBSHIRANI, R. (2010). Regularization paths for generalized linear models via coordinate descent. *Journal of Statistical Software* **33** 1-22.
- GABAY, D. and MERCIER, B. (1976). A dual algorithm for the solution of nonlinear variational problems via finite element approximation. *Computer and Mathematics with Applications* **2** 17-40.
- GREEN, P. J. and SILVERMAN, B. W. (1994). *Nonparametric regression and generalized linear model: a roughness penalty approach*. Chapman and Hall.
- GUO, J., JAMES, G., LEVINA, E., MICHAELIDIS, G. and ZHU, J. (2010). Principal component analysis with sparse fused loadings. *Journal of Computational and Graphical Statistics* **19** 930-946.
- HANNACHI, A., JOLLIFFE, I. T. and STEPHENSON, D. B. (2007). Empirical orthogonal functions and related techniques in atmospheric science: A review. *International Journal of Climatology* **27** 1119-1152.
- HONG, Z. and LIAN, H. (2013). Sparse-smooth regularized singular value decomposition. *Journal of Multivariate Analysis* **117** 163-174.
- HUANG, J. Z., SHEN, H. and BUJA, A. (2008). Functional principal components analysis via penalized rank one approximation. *Electronic Journal of Statistics* **2** 678-695.
- JOLLIFFE, I. T. (1987). Rotation of principal components: Some comments. *Journal of Climatology* **7** 507-510.
- JOLLIFFE, I. T. (2002). *Principal component analysis*. Wiley Online Library.
- JOLLIFFE, I. T., UDDIN, M. and VINES, S. K. (2002). Simplified EOFs—three alternatives to rotation. *Climate Research* **20** 271-279.
- KANG, E. L. and CRESSIE, N. (2011). Bayesian Inference for the Spatial Random Effects Model. *Journal of the American Statistical Association* **106** 972-983.
- KARHUNEN, K. (1947). Über lineare methoden in der Wahrscheinlichkeitsrechnung. *Annales Academiae Scientiarum Fennicae Series A* **37** 1-79.

- LOÈVE, M. (1978). *Probability theory*. Springer-Verlag, New York.
- LU, Z. and ZHANG, Y. (2012). An augmented Lagrangian approach for sparse principal component analysis. *Mathematical Programming* **135** 149–193.
- RAMSAY, J. O. and SILVERMAN, B. W. (2005). *Functional data analysis*, 2nd ed. New York: Springer.
- RICHMAN, M. B. (1986). Rotation of principal components. *Journal of Climatology* **6** 293-335.
- RICHMAN, M. B. (1987). Rotation of principal components: A reply. *Journal of Climatology* **7** 511–520.
- SHEN, H. and HUANG, J. Z. (2008). Sparse principal component analysis via regularized low rank matrix approximation. *Journal of Multivariate Analysis* **99** 1015-1034.
- TIBSHIRANI, R. (1996). Regression shrinkage and selection via the Lasso. *Journal of the Royal Statistical Society. Series B* **58** 267-288.
- TZENG, S. and HUANG, H.-C. (2015). Non-stationary multivariate spatial covariance estimation via low-rank regularization. *Statistical Sinica* **26** 151-172.
- YAO, F., MULLER, H.-G. and WANG, J.-L. (2005). Functional data analysis for sparse longitudinal data. *Journal of the American Statistical Association* **100** 577-590.
- ZOU, H., HASTIE, T. and TIBSHIRANI, R. (2006). Sparse principal component analysis. *Journal of Computational and Graphical Statistics* **15** 265-286.